Available online at www.sciencedirect.com
SCIENCE DIRECT
Polymer 46 (2005) 10493–10505
polymer
www.elsevier.com/locate/polymer

New insights on the solution behavior and self-assembly of polystyrene/poly(2-vinylpyridine) 'hairy' heteroarm star copolymers with highly asymmetric arms in polar organic and aqueous media

Miroslav Štěpánek[a], Pavel Matějíček[a], Jana Humpolíčková[a], Jitka Havránková[a], Klára Podhájecká[a], Milena Špírková[b], Zdeněk Tuzar[b], Constantinos Tsitsilianis[c,d], Karel Procházka[a,*]

[a]*Department of Physical and Macromolecular Chemistry and Laboratory of Specialty Polymers, School of Science, Charles University in Prague, Albertov 2030, 12840 Prague 2, Czech Republic*
[b]*Institute of Macromolecular Chemistry, Academy of Sciences of the Czech Republic, Heyrovský Square 2, 16206 Prague 6, Czech Republic*
[c]*Department of Chemical Engineering, University of Patras, 26504 Patras, Greece*
[d]*Institute of Chemical Engineering and High-Temperature Chemical Processes, ICE/HT-FORTH, 26504 Patras, Greece*

Received 16 February 2005; received in revised form 20 June 2005; accepted 9 August 2005
Available online 13 September 2005

Abstract

The solution behavior and self-assembly of a 'hairy' heteroarm star copolymer polystyrene/poly(2-vinylpyridine) containing 20 fairly short polystyrene and 20 long poly(2-vinylpyridine) arms was studied in 1,4-dioxane–methanol mixtures and in acidic aqueous solutions. The copolymer forms reversible micelles in 1,4-dioxane–methanol mixtures. Since the conformation of the unimolecular heteroarm star (unimer) with collapsed insoluble PS arms and stretched soluble PVP arms resembles the spherical core/shell micelle, the solubility of the copolymer in the selective solvent is fairly high and the multimolecular micelles are formed by only few heteroarm stars. Both heteroarm stars (in pure 1,4-dioxane) and micellar systems (composed of both micelles and unimolecular heteroarm stars (unimers) in 1,4-dioxane–methanol mixtures) may be transferred in acidic aqueous media by dialysis. Polyelectrolyte behavior of unimer stars was studied in detail in acidic aqueous media. Static and dynamic light scattering measurements show that heteroarm stars interact electrostatically over long distances in low ionic strength solutions. Experimental data indicate that the charged stars may form temporary shell interacting (electrostatically stabilized) aggregates at elevated concentrations.

Keywords: Heteroarm star copolymers; Self-assembly; Polyelectrolytes

1. Introduction

Heteroarm (also referred miktoarm) star copolymers are important polymeric materials with interesting architecture that form a variety of nanosegregated structures both in solutions [1–8] and in solid state (bulk and on surfaces) [9–15] and offer a number of potential applications. The conformations of heteroarm stars, their self-assembly, rheology of their melts and solutions, etc. have been a subject of numerous experimental and theoretical studies in recent years. The solution behavior resembles that of linear diblock copolymers [16–25] rather than linear multiblock copolymers. Heteroarm stars with a low number of arms of two types usually associate in selective solvents, i.e. in good solvents for one type of arms, which are precipitants for the other type and form multimolecular core/shell micelles. The association number is lower than that of linear diblock copolymers with the same ratio of monomer units and decreases with increasing number of soluble arms [3,6,7]. Moreover, their critical micelle concentration is significantly higher and therefore, they tend to form unimolecular micelles in dilute solutions in selective solvents [3,6,7].

'Hairy' multiarm stars with asymmetric arms of different type resemble polymeric micelles. Therefore, unimer stars

* Corresponding author. Tel.: +420 221 951293; fax: +420 224 919752.
E-mail address: prochaz@vivien.natur.cuni.cz (K. Procházka).

0032-3861/$ - see front matter © 2005 Elsevier Ltd. All rights reserved.
doi:10.1016/j.polymer.2005.08.031

with collapsed insoluble and expanded soluble arms may exist in selective solvents in appreciable concentrations, depending on temperature, relative length and number of different arms [4,15].

In an earlier paper, we studied the self-assembly of polystyrene/poly(2-vinylpyridine) heteroarm star copolymers, PS(n, L_1)–PVP(n, L_2), differing in numbers (n) and lengths (L_1 and L_2) of arms [4]. The light scattering study revealed very interesting behavior of the 'hairy' PS(20, 3k)–PVP(20, 23k) copolymer (Fig. 1). In this paper, we study the self-assembly of this sample and its solution behavior in 1,4-dioxane–methanol mixtures and in low ionic strength aqueous media in detail. We focus mainly (i) on reversible micellization in binary 1,4-dioxane–methanol mixtures and (ii) on frozen micelles in acidic water prepared via dialysis from binary solvent mixtures.

In order to avoid any possible confusion, we would like to make one comment concerning the nomenclature used. For the non-associated (i.e. monomeric) heteroarm star we will use either the term unimer in connection with the mobile or kinetically frozen unimer–micelle equilibrium, or heteroarm star in connection with its structural characteristics. The term 'micelle' will be used for the core/shell structures with compact PS cores, while the general term 'associate' will be used mainly for loose shell-interacting associates that we observe at elevated concentrations in low ionic strength media.

2. Experimental procedures

2.1. Materials

The PS(20, 3k)–PVP(20, 23k) star copolymer was prepared via anionic polymerization using three-step sequential 'living' copolymerization procedure. In the first step, the PS arms were synthesized a number n ca. 20 of which were joined together in the second step by reacting the living PS chains with a small amount of divinylbenzene. The number of PS arms is controlled by the mass ratio of living PS arms to divinylbenzene. A star-shaped polystyrene was thus formed, bearing a number of active sites at poly(divinylbenzene) core which is equal to the number of the attached PS arms. In the third step, a second generation of PVP arms grows from the cores on adding vinylpyridine to the reaction medium.

The sample has been characterized by static light scattering, size exclusion chromatography and ^{1}H NMR. The weight-average molar masses of the copolymer and of PS and PVP arms are 5.29×10^5, 3.0×10^3 and 22.8×10^3 g/mol, respectively. Details on the synthesis and characterization are given in Ref. [1]. The measurement of apparent weight average molar mass, M_w and SEC analysis confirmed the values reported earlier [4]. The SEC elution curve is shown in Fig. 2. The polydispersity based on the polystyrene (linear chain) calibration is $M_w/M_n = 1.24$.

The PS(20, 3k)–PVP(20, 23k) micelles in dioxane, methanol and dioxane–methanol mixtures were prepared by direct dissolution of the copolymer in the solvent. The aqueous solutions of PS(20, 3k)–PVP(20, 23k) micelles were prepared in two steps: (i) Copolymer solutions in organic solvents were swiftly mixed with equivalent volumes of 0.01–0.1 M aqueous HCl under vigorous stirring. (ii) The organic solvent was removed by extensive dialysis of micellar solutions against 0.01–0.1 M aqueous HCl.

For studies of the polyelectrolyte behavior, a relatively concentrated solution of unimer micelles (ca. 10 mg/ml) in 0.01 M HCl was prepared by dialysis from 1,4-dioxane. The solution was dialyzed several times against an excess of aqueous HCl solution with different concentrations to get solutions with required pH. The dialysis was performed in PET bottles to prevent the contamination of aqueous solutions by small alkaline ions.

2.2. Techniques

The light scattering setup (ALV, Langen, Germany) consists of a 633 nm He–Ne laser, an ALV CGS/8F goniometer, an ALV High QE APD detector and an ALV 5000/EPP multibit, multitau autocorrelator [25]. The solutions for measurements were filtered through 0.45 μm

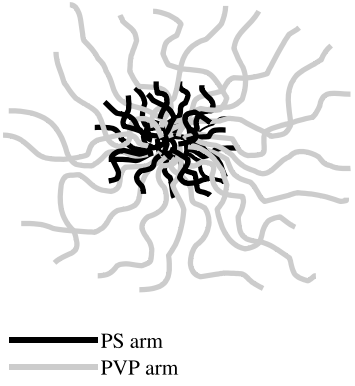

Fig. 1. A PS(20, 3k)–PVP(20, 23k) star copolymer molecule in a good solvent for both types of arms.

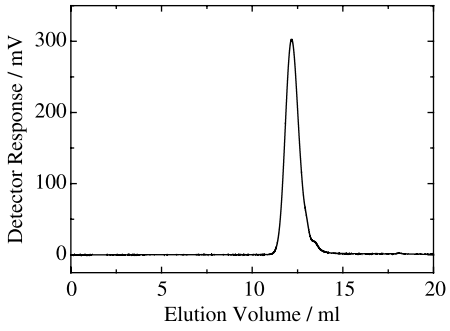

Fig. 2. SEC elution curve of PS(20, 3k)–PVP(20, 23k) star copolymer.

Acrodisc filters. The measurements were carried out for different concentrations (0.5–30.0 mg/ml) and different angles at 20 °C. The measurements for the low ionic strength solutions were performed in quartz cells.

The data analysis of dynamic light scattering (DLS) measurements was performed by fitting the measured normalized autocorrelation function $g_2(t)=1+\beta|g_1(t)|^2$, where $g_1(t)$ is the electrical field correlation function, t is the lag-time and β is a factor accounting for deviation from the ideal correlation. An inverse Laplace transform of $g_1(t)$ with the aid of a constrained regularization algorithm (REPES) [26] provides the distribution of relaxation times, $\tau A(\tau)$

$$g_1(t) = \int \tau A(\tau)\exp\left(\frac{-t}{\tau}\right)\mathrm{d}\ln\tau \tag{1}$$

Diffusion coefficients were calculated from individual diffusion modes as $D=\Gamma/q^2$, where $\Gamma=1/\tau$ and $q=(4\pi n_0/\lambda)\sin(\theta/2)$ is the magnitude of the scattering vector. Here θ is the scattering angle, n_0 the refractive index of pure solvent and λ the wavelength of the incident light. Hydrodynamic radii, R_H, were evaluated from the diffusion coefficients using the Stokes–Einstein formula, $R_H=kT/(6\pi D\eta)$. The viscosity and refractive index of 1,4-dioxane–methanol mixtures for the evaluation of R_H values were taken from Ref. [27].

The static light scattering (SLS) measurements data were treated by the standard Zimm method using the equation [28]

$$\frac{Kc}{R^{\mathrm{cor}}(q,c)} = \frac{1}{p(q,c)M_w} + 2A_2c + \ldots \tag{2}$$

where $K=4\pi^2n^2(\mathrm{d}n/\mathrm{d}c)^2/\lambda^4N_A$ is a constant containing the refractive index n of the solvent, refractive index increment of the polymer with respect to the solvent, $(\mathrm{d}n/\mathrm{d}c)$, wavelength of the incident light, λ, and the Avogadro constant, N_A. The other symbols stand for: $R^{\mathrm{cor}}(q,c)$ is the corrected Rayleigh ratio which depends on the polymer concentration and on the scattering vector q, M_w is the apparent weight average molar mass of scattering polymeric particles and A_2 is the 'light-scattering-weighted' second virial coefficient of the concentration expansion.

The function $p(q,c)=I^{\mathrm{cor}}(q)/I^{\mathrm{cor}}(q=0)$ takes into account both the intraparticle and interparticle interference effects. We assume that the scattering function $p(q,c)$ may be reasonably expressed as a product of the single particle form factor $P(q)$, and the solution structure factor $S(q,c)$, i.e. $p(q,c)=P(q)S(q,c)$ [29]. Because polystyrene and poly(2-vinylpyridine) are isorefractive polymers, the apparent weight average molar mass M_w of a PS–PVP copolymer is very close to the true molar mass, even for samples that are polydisperse in molar masses and heterogeneous in composition. However, the analysis of our sample indicates that it is a fairly uniform copolymer as concerns both characteristics.

The refractive index increments, $\mathrm{d}n/\mathrm{d}c$, were taken from the literature [30]. The situation is simplified by the fact that polystyrene and poly(2-vinylpyridine) are isorefractive polymers and the refractive index increment in 1,4-dioxane is $\mathrm{d}n/\mathrm{d}c=0.171$ for both homopolymers. For PS in water, we use the literature value for PS latexes, $\mathrm{d}n/\mathrm{d}c=0.257$ and for PVP in methanol, $\mathrm{d}n/\mathrm{d}c=0.254$. Since the refractive indexes of methanol and water are similar, we assume that the same values may be used for PS in methanol and PVP in water. Increments in mixed 1,4-dioxane–methanol solvents were calculated using the values of increments in pure solvents and the experimental curve of the refractive index n as a function of the solvent composition [27]. This approximation may cause an error of several percents in molar masses, which is acceptable for association studies in non-electrolyte systems. In measurements of the polyelectrolyte behavior, the solvent from the dialysis bath was used for diluting the solutions to keep the osmotic and optical properties of the solvent constant.

Fluorescence correlation spectroscopy (FCS) measurements were performed with a binocular microscope ConfoCor I, Carl Zeiss, Germany, equipped with a 514 nm argon laser, an adjustable pinhole together with a special fluorescence optics, SPCM-200PQ detection diode and an ALV-5000 correlator (ALV, Langen, Germany). The normalized autocorrelation function of fluctuations, which is used for the evaluation of the diffusion coefficient is given by the following equation [31]

$$G(\tau) = 1 + \frac{\langle F(t)F(t+\tau)\rangle}{\langle F(t)\rangle^2} \tag{3}$$

where $F(t)$ is the fluorescence intensity in time t and $F(t+\tau)$ is the intensity in time $t+\tau$ and the averaging is performed through the whole measured time interval. According to current experimental conditions, a roughly cylindrical volume ca. 10^{-16} l is irradiated by a focused laser beam with Gaussian intensity profile. This small volume contains up to 10 fluorescent molecules and fluctuations in fluorescence intensity are caused mainly by the diffusion of fluorescent molecules in and out of the irradiated volume. Since the intensity of the focused beam is very high, the photobleaching must be always taken into account as a complicating process (even for strongly photobleaching-resistent probes). Using different models differing in complexity [31,32], the diffusion coefficient of the fluorescently labeled macromolecules, D, may be obtained from the characteristic diffusion time τ_F, which is necessary for the freely diffusing labeled macromolecule to reach an average distance corresponding to the dimensions of the irradiated volume. Then the hydrodynamic radius of diffusing particles can be evaluated similarly to DLS.

Atomic force microscopy (AFM) measurements were performed in the tapping mode under ambient conditions using a commercial scanning probe microscope, Digital Instruments Nanoscope dimensions 3, equipped with a

Nanosensors silicon cantilever, typical spring constant 40 N m^{-1}. Details of the measurement and the principle of the evaluation of micellar polydispersity were given in our earlier paper [25]. Polymeric micelles were deposited on a fresh (i.e. freshly peeled out) mica surface (flogopite, theoretical formula $KMg_3AlSi_3O_{10}(OH)_2$, Geological Collection of Charles University in Prague, Czech Republic) by a fast dip coating in a dilute micelle solution in 0.01 M HCl (c ca. 10^{-2} g l^{-1}). After the evaporation of water, the samples for AFM were dried in vacuum oven at ambient temperature for ca. 5 h.

Steady-state fluorescence spectra were measured in 1 cm quartz cuvettes using a SPEX Fluorolog 3-11 fluorometer. Time-resolved fluorescence decays were measured by means of the time-correlated single photon counting technique on an Edinburgh Instruments ED 299 T fluorometer equipped with a hydrogen-filled nanosecond coaxial discharge flashlamp (half-width of the pulse ca. 1.2 ns) [24]. The measured decays were fitted to the convolution of multiexponential functions with the instrument response profile using the Marquardt–Levenberg nonlinear least squares method.

The pH measurements were performed with a Radiometer PHM 93 reference pH meter equipped with a PHC 3006 combined glass microelectrode. Viscosities were measured at 20 °C with a standard Ubbelohde viscometer.

Size exclusion chromatography (SEC) analysis was carried out on a TSP (Thermo Separation Products, Florida, USA) chromatograph fitted with a UV detector operating at 254 nm. A series of two PL-gel columns (Mixed-B and Mixed-C, Polymer Laboratories Bristol, UK) and THF (flow rate 0.7 ml/min) were used. Molar masses are reported relative to polystyrene standards.

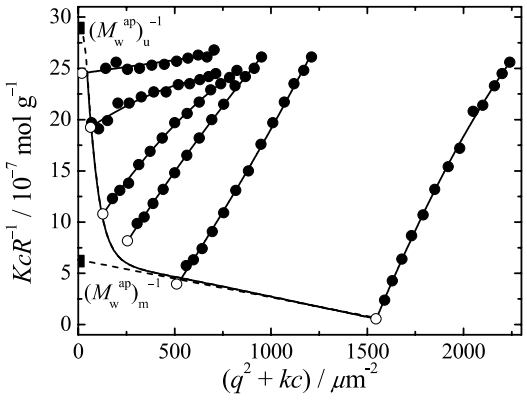

Fig. 3. Zimm plot for SLS from PS(20, 3k)–PVP(20, 23k) solutions in 1,4-dioxane–methanol (50 vol%) mixture. The open circles represent the extrapolated dependence of $Kc/R^{cor}(q=0,c)$ on the copolymer concentration, c. The figure also shows two values of reciprocal molar mass, M_w^{-1}, obtained from the $Kc/R^{cor}(q=0,c)$ vs. c dependence extrapolations to zero concentration in the high (multimolecular micelles, $(M_w)_m^{-1}$) and low (unimer micelles, $(M_w)_u^{-1}$) concentration region. The plot constant k is 200 μm^{-2} l g^{-1}.

3. Results and discussion

3.1. Static and dynamic light scattering study

First we studied the behavior of unimers and micelles in a relatively broad concentration region (up to 30 g/l) in the binary mixture 1,4-dioxane–methanol. 1,4-dioxane is a good solvent for both polystyrene and poly(2-vinylpyridine) and the sample dissolves well in the form of unimers. Methanol is a strong precipitant for polystyrene and a fairly good solvent for non-protonized PVP. In mixtures with increasing methanol content, the solvent quality deteriorates for PS. In mixtures with ca. 20 vol% of methanol, the PS arms become insoluble and the solubility of PVP arms, even though fairly high, is no more sufficient to keep the unimer in the solution. Several stars associate and form reversible micelles with swollen PS cores. In our earlier studies, we found that the core-forming PS arms are partially intermixed with relatively stretched PVP arms as a consequence of copolymer architecture [4]. Some theoretical studies and computer simulations suggest that the star copolymer conformations do not have to be strictly sphero-symmetrical and that the core might be displaced from the center of gravity in order to minimize the intermixing of arms of different types, but the asymmetry and the separation of gravity centers of PVP and PS blocks are rather small [33].

The reversible micellization of the hairy heteroarm copolymer in 1,4-dioxane–methanol mixtures is well documented by static and dynamic light scattering measurements. Fig. 3 shows the Zimm plot for PS(20, 3k)–PVP(20, 23k) copolymer in a mixture of 1,4-dioxane with 50% of methanol in a relatively broad concentration region. Even though the analysis of the Zimm plots of associating polymers is not as straightforward as in the case of well-behaving molecularly dissolved polymers, this type of presentation is a comprehensive legitimate way of presenting SLS data and shows immediately irregularities and suggests possible reasons of the observed behavior. For reversibly associating systems, an appropriate analysis was developed by Elias long time ago [34]. Since the weight average molar mass, $M_w^{app} = w_U M_U + w_M M_M$ (where w_i are the weight fractions and subscripts U and M stand for unimer and micelles, respectively) increases above critical micelle concentration (cmc), the $Kc/R^{cor}(q=0,c)$ curve decreases and it levels-off in the region of high polymer concentrations (or continues linearly, if the second virial coefficient A_2 differs significantly from zero). For typical micellizing systems at high concentrations, it holds, $w_M \gg w_U$ and $M_M \gg M_U$. Therefore, the apparent molar mass obtained from the linear high concentration region is close to that of micelles, i.e. $M_w^{app} \approx M_M$. The plot of experimental $Kc/R^{cor}(q=0,c)$ values, extrapolated to the zero scattering vector q, as a function of c shows a well pronounced decreasing sigmoidal curve which is typical for the reversible association and the comparison with DLS data (see further) supports this conclusion [16–18]. Since the star

architecture promotes the solubility of the copolymer in selective solvents for PVP, the association number is low and the critical micelle concentration (cmc) is high (and therefore, detectable by SLS) in comparison with micelles formed by linear block copolymers. The Zimm plots for other mixtures are similar to that shown in Fig. 3. The association number generally increases and micellar cores shrink with increasing content of CH_3OH in the mixed solvent. The critical micelle concentration is actually detectable (although not accurately measurable) only in 1,4-dioxane-rich solvents. In these solvents, the extrapolation of $Kc/R^{cor}(q,c)$ to zero q and zero c verges towards the unimer star molar mass, $(M_w)_u$. For heteroarm stars, the multimolecular micelles in 1,4-dioxane-rich mixtures contain only few copolymers and the apparent molar mass of micelles, $(M_w)_m$, cannot be measured accurately by SLS. Nevertheless, it still can be roughly estimated using linear extrapolation of the 'envelope' curve (i.e. that for zero q, see Fig. 3 from the high concentration region. The procedure yields the association number close to 4. Hence we assume the coexistence of unimers and associates (on average tetramers) in reversible equilibrium. The reversible association mechanism is well documented by DLS measurements. Fig. 4(a) shows the distribution of relaxation times measured at different concentrations. The positions of both peaks do not shift with copolymer concentration. The fraction of multimolecular micelles (the area of the peak around 1 ms) increases with increasing polymer concentration. Angular measurements (Fig. 4(b)) prove that the observed relaxation times correspond to the diffusion of both species. Since the positions of peaks do not basically shift with concentration, we think that the association obeys, in principle, the closed association model, but relatively broad peaks indicate the distribution of association numbers. This is a reasonable observation, because the association numbers are assumed to satisfy the Poisson distribution, which is fairly broad for low mean values and narrow for high ones when related to the mean value.

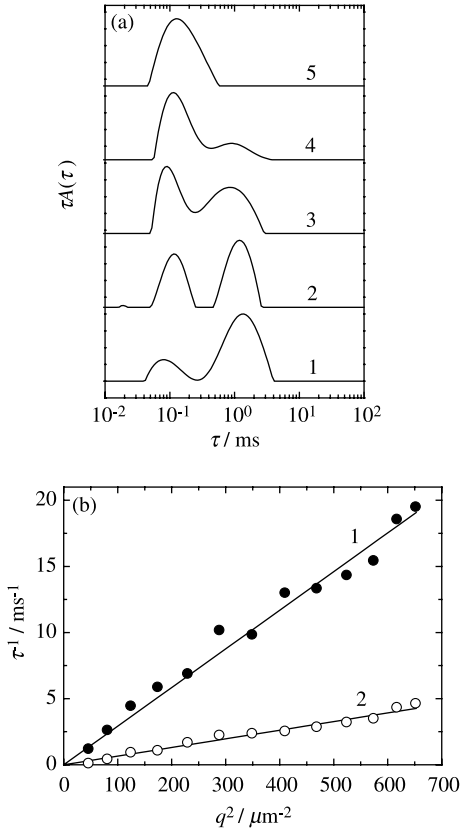

Fig. 4. (a) Relaxation time distributions of DLS from PS(20, 3k)–PVP(20, 23k) solutions in 1,4-dioxane–methanol(50 vol%) mixture, measured at scattering angle $\theta = 90°$. The copolymer concentrations are 10.20 (curve 1), 5.10 (curve 2), 2.55 (curve 3), 1.28 (curve 4) and 0.32 g/l (curve 5). (b) Reciprocal mean relaxation time, τ^{-1}, of fast (curve 1) and slow (curve 2) mode for 1.28 g/l solution as a function of q^2.

The apparent weight average molar mass of polymeric particles, M_w^{app}, (obtained by extrapolation from the high concentration region) is shown in Fig. 5 (curve 1) as a function of solvent composition. In mixtures with 0–80% of methanol, M_w^{app} increases only little. A substantial increase in M_w^{app} is observed only in methanol-rich mixtures. Curve 2 shows the apparent radius of gyration, R_g^{app} of associates as a function of solvent composition. The R_g^{app}-values were obtained from tangents of angular dependences $Kc/R^{cor}(q,c)$ vs. q^2 (for $q \to 0$) in the 'linear' high concentration region. Since the experimental radius of gyration measured by SLS is the z-average value, it is fairly close to that of associates in the 'linear' high concentration region. It should be noted that in solvents with 80–100 vol% of methanol, cmc is very low and is not detectable and only the linear parts of concentration dependences of $Kc/R^{cor}(q = \text{const},c)$ are measurable and the Zimm plots look fairly regular yielding directly characteristics of micelles. The R_g^{app}-dependence on the solvent composition is non-monotonous. A combination of two effects: (a) increasing molar masses of reversible mutimolecular micelles and (b) decreasing size of their insoluble PS cores with increasing content of CH_3OH results in the dependence of R_g^{app}, which passes a maximum for solvent composition ca. 50 vol% of methanol (curve 2), decreases in the region 50–80 vol% of methanol and then

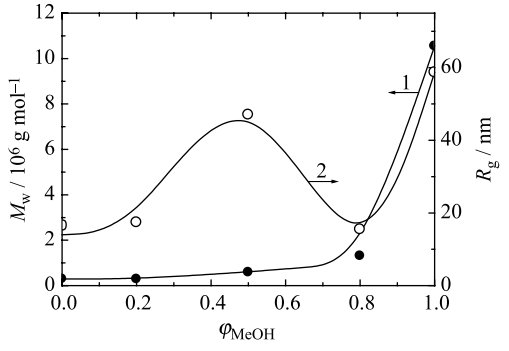

Fig. 5. Molar mass, M_w (curve 1) and radius of gyration, R_g (curve 2), obtained from SLS from the PS(20, 3k)–PVP(20, 23k) solutions in 1,4-dioxane–methanol mixtures as a function of methanol volume fraction, ϕ_{MeOH}.

rises again in methanol-rich mixtures. At first, relatively loose micelle-like associates form, the cores of which shrink with increasing content of methanol.

We did not study the association behavior of PS(20, 3k)–PVP(20, 23k) sample in pseudo-ternary 1,4-dioxane–methanol–acidic water (0.1 M HCl) solvent mixtures systematically. In this paper, we only compare light scattering data in 1,4-dioxane–methanol mixtures with those transferred by dialysis in acidic aqueous media. In our earlier studies, we found that poly(2-vinylpyridine) is soluble in water at pH lower than 4.8 and at higher pH, the deprotonized PVP precipitates [4,19]. An increase in the content of 0.1 M aqueous HCl sharply deteriorates solvent quality for PS and improves solubility of protonized PVP (as compared with non-protonized PVP in methanol). Micellar cores shrink and continuously kinetically freeze in critical 1,4-dioxane–methanol–0.1 M aqueous HCl mixtures, the water fraction of which decreases with increasing methanol content in the original 1,4-dioxane–methanol mixture.

The apparent weight average molar masses, M_w^{app} and apparent radii of gyration of kinetically frozen micelles in acidic water are shown in Fig. 6 as functions of composition of the binary 1,4-dioxane–methanol solvent, from which the micelles were quenched in acidic water (curves 1 and 2, respectively). Aqueous mixtures prepared from dilute solutions in binary solvents with 20–80 vol% CH_3OH contain both unimers and multimolecular micelles, which agrees with our earlier observations [4]. When the Zimm plots and apparent molar masses, M_w^{app}, of micellar systems in acidic water are compared with those in original binary mixtures, it is evident that the unimer/micelle equilibrium existing in binary mixtures has been basically preserved (trapped in a kinetically frozen state). The kinetically frozen unimers and associates behave as independent species in acidic water. Their mass ratio depends on copolymer concentration and on composition of the original binary mixture, but it does not almost change with concentration of final aqueous solution. It means that unimers with collapsed PS arms and stretched protonized PVP arms do neither

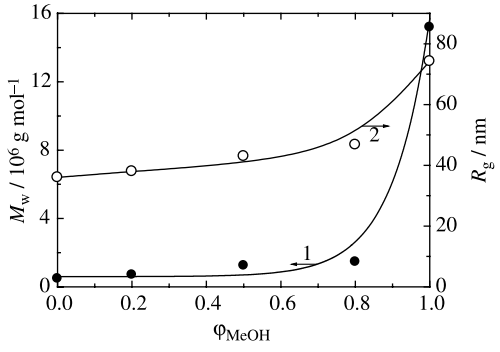

Fig. 6. Molar mass, M_w (curve 1), radius of gyration, R_g (curve 2), obtained from SLS from PS(20, 3k)–PVP(20, 23k) solutions in 0.1 M HCl as a function of methanol volume fraction, ϕ_{MeOH}, in the starting solution in 1,4-dioxane–methanol mixture.

associate nor precipitate, but they survive the transfer in aqueous medium.

Since the PS cores are collapsed in water, the apparent radii of gyration, R_g^{app}, are small for systems prepared from 1,4-dioxane-rich binary solvent mixtures and increase only in the region of high methanol contents. The copolymer dissolves also in methanol and forms relatively compact micelles with a fairly high molar mass (Fig. 5). These high-molar-mass micelles may be also transferred in 0.1 M HCl without appreciable changes in molar mass.

It is worth-mentioning that it is possible to transfer pure unimers without almost any aggregation or appreciable changes in polydispersity directly from 1,4-dioxane to acidic water by adding an excess of acidic water and dialyzing against 0.1 M aqueous HCl. This is due to the fact that the copolymer architecture with short insoluble PS arms and long soluble protonized PVP arms promotes the solubility of the unimer in acidic aqueous media.

The second part of the light scattering study was devoted to the behavior of PS(20, 3k)–PVP(20, 23k) in low ionic strength aqueous media. Recently, we studied the behavior of multimolecular polystyrene-*block*-poly(methacrylic acid) micelles, PS–PMA, in aqueous media and we found fairly surprising polyelectrolyte behavior in low ionic strength solutions [35]. We found that fairly many counter-ions escape from the shell in the solution at pH close to effective pK_A and do not efficiently screen electrostatic interactions. In this respect, the shell resembles more the Pincus brush [36,37] than the osmotic brush [38–41] and PS–PMA micelles behave as charged nanoparticles and interact strongly over long distances. With increasing ionic strength, or at higher pH, when the dissociation is enhanced, a gradual transition to the salted brush regime was observed. Since PMA is not a typical weak polyelectrolyte and its behavior resembles in many respects to that of polysoaps [42–45], we were interested if PS–PVP stars with partially protonized and positively charged PVP arms behave similarly.

We studied the behavior of salt-free micellar solutions in a fairly broad concentration region under strictly controlled conditions. Firstly, we estimated the degree of protonization of unimer stars in salt free solutions as a function of pH (adjusted by the addition of HCl). The principle of the measurement was explained in our earlier paper [4]. It consists in a combination of dialysis and alkalimetric titration. When micelles with PVP shell are dialyzed many times against a large excess of solution with known HCl concentration (and pH), finally, i.e. after several exchanges of the dialysation bath, the dilute micellar solution acquires precisely the same concentration of HCl as the dialysation bath, but besides HCl, it contains also micelles with partially (equilibrium) protonized PVP shells. The alkalimetric titration allows the evaluation of the degree of PVP protonization. The obtained curve is reproduced in Fig. 7. The results agree with our earlier measurements on multimolecular micelles. The protonization is very low at

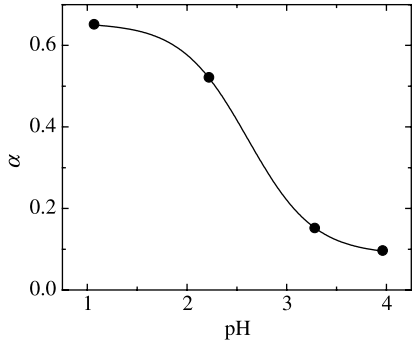

Fig. 7. Degree of protonization, α, of poly(2-vinylpyridine) in the PS(20, 3k)–PVP(20, 23k) micelles (copolymer concentration $c=9.66$ g/l) dissolved in aqueous HCl solutions, as a function of pH. The aqueous solutions were prepared from the solution in 1,4-dioxane.

pH 4 where PVP chains start to dissolve (pH$<$4.8) and hence the electric charge on the star is small and the charge density is low. The degree of protonization increases from ca. 0.2–0.5 between pH 3 and 2, and is still less than 0.7 at pH 1. Because the number of chargeable groups is limited, the charge density is low in pH region 2–4. The electrostatic forces are weak and counterions escape in bulk solution due to entropy reasons [35–37]. Individual PS–PVP heteroarm stars behave as effectively charged particles and interact electrostatically over long distances.

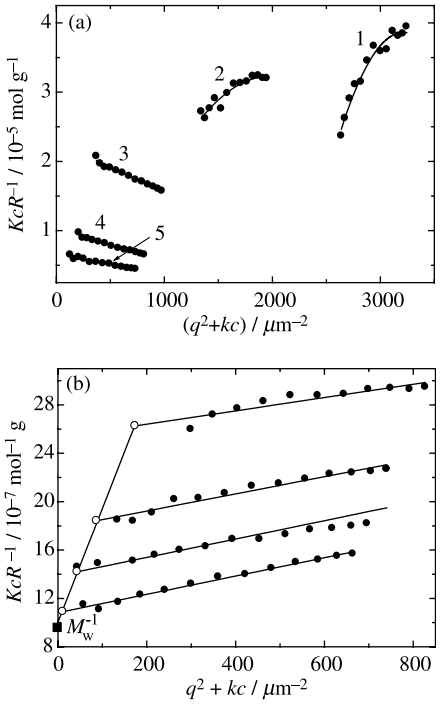

Fig. 8. Zimm plots for the SLS from the PS(20, 3k)–PVP(20, 23k) solutions in (a) 10^{-4} and (b) 10^{-1} M HCl prepared from the solution in 1,4-dioxane. Concentrations of the solutions in (a) (curves 1–5) are 8.64, 4.32, 1.08, 0.54 and 0.27 g/l, respectively. The open circles and the solid square in (b), respectively, represent the extrapolated dependence of $Kc/R^{cor}(q=0,c)$ on the copolymer concentration, c, and the value of reciprocal molar mass, M_w^{-1}, obtained from the $Kc/R^{cor}(q=0,c)$ vs. c dependence extrapolation to zero concentration. The plot constants k are (a) 300 and (b) 50 μm^{-2} l g^{-1}.

The electrostatic interactions are well manifested by light scattering measurements. Fig. 8(a) shows SLS data for unimer stars prepared in 10^{-4} M HCl. We present the data in the form of the Zimm plot, which, as already mentioned, immediately reveals all irregularities in the behavior. The Zimm plot was constructed in the concentration range from 0.25 to 9 g/l. Angular dependences of $Kc/R^{cor}(q,c)$ for low concentrations are negative due to important electrostatic interactions. However, in the high concentration region, the slope vs. q^2 changes and becomes positive indicating 'different sort of behavior' and possible formation of aggregates or in homogeneities on the 10^1–10^2 nm scale. The change in the sign of the slope occurs in the concentration region, where the stars with fully stretched PVP arms would touch each other (precisely, slightly bellow the overlap of 'geometrical' equivalent spheres, i.e. slightly below c^*). Average distances between individual stars estimated on the basis of the uniform arrangement are ca. 62 and 40 nm for $c=4.3$ and 8.6 g/l, respectively. Such distances are comparable with the contour length of two PVP arms (ca. 55 nm). It is not easy to interpret the precise physical meaning of the slope. We believe that the highly positive slopes may be attributed to fluctuations of less and more concentrated domains, representing loose aggregates of stars stabilized by counterions, because close to the overlap concentration, the formation of temporary shell-interpenetrating aggregates (stabilized by the cloud of common counter-ions compensating the charge) cannot be precluded in 'amphiphic' systems containing poorly soluble collapsed PS arms only partially protected by a scarce shell of soluble PVP arms. Hence we use the descriptive term 'apparent radius of gyration' for brevity, even though a more general (but less descriptive) term 'correlation length of fluctuations' based on the Ornstein-Zernike approach [46] may seem more appropriate. The apparent radii of gyration, R_g^{app}, increase with increasing concentration (R_g are 49 and 84 nm for two highest concentrations, $c=4.3$ and 8.6 g/l, respectively). In any case, it is necessary to keep in mind that even for real interacting particles neither the initial slopes, nor the entire curves provide correct radii of gyration, R_g^{app} nor particle functions, $P(q)$, respectively. The measured q-dependence is a result of the interplay between the particle function, $P(q)$ and the structure factor, $S(q,c)$. It is worth-mentioning that also the viscosity of the most concentrated low ionic strength solution is quite high and both DLS and FCS measurements provide very long diffusion-controlled relaxation times (see the next part).

In 10^{-2} M HCl, the protonization of PVP is significantly promoted, but the electrostatic interactions are not yet screened. The region of viscous solutions with positive slopes of q^2-dependences of $Kc/R^{cor}(q,c)$ expands to fairly low concentrations, which indicates strong electrostatic interaction at relatively low concentrations (not shown). In 0.1 M HCl, the concentration of small ions is fairly high and electrostatic interactions are screened. SLS measurement yields the regular Zimm plot (Fig. 8(b)). The viscosity of

the most concentrated solution is very low, i.e. it is comparable with that of water. The experimental value of the apparent molar mass, $M_w = 8.4 \times 10^5$ g/mol corresponds roughly to that of unimer in 1,4-dioxane. It is slightly higher, probably due to low admixture of aggregates (see later). The plot gives a reasonable value of the apparent gyration radius ca. 40 nm and the second virial coefficient is positive, $A_2 = 1.35 \times 10^{-7}$ mol l g^{-2} reflecting a good solubility of protonized PVP arms in 0.1 M HCl.

DLS data (Figs. 9 and 10) for low ionic strength solutions are interesting. In all cases, the measurement yields a single relaxation mode. Angular dependences (insert in Fig. 10) show that the observed relaxation corresponds basically to the diffusion of particles, i.e. the product τq^2 is almost constant. The observed relaxation times depend on ionic strength of the solution and increase strongly with polymer concentration. In considerably interacting systems with I around 10 mmol/l, they provide very large apparent hydrodynamic radii, R_H^{app}. Even though the observed R_H^{app} values do not reflect the real size of aggregates, the measurements support the conclusions drawn from SLS measurements. It seems that at 'higher concentrations', i.e. starting at 1 g/l, the stars with partially ionized and stretched PVP chains form reversible aggregates temporarily stabilized by a common cloud of counter-ions. The average lifetime of aggregates has to be appreciably long in comparison with measured relaxation times. Otherwise the measurement would not reflect the motion of aggregated structures and faster relaxation times of different origin should be detected. The DLS relaxation times correlate with viscosity of the electrostatically interacting heteroarm stars in aqueous solution. In Fig. 9, viscosity (curve 1) is compared with the relaxation time τ (curve 2, measured at 90°) as a function of pH. Both curves pass maximum in the same HCl concentration region.

In low ionic strength solutions, the measured relaxation times are very long and increase steeply with polymer concentration (Fig. 10, curve 1). It is interesting that we do not observe fast relaxation modes, i.e. we do not see the motion of non-aggregated stars. A correct interpretation of

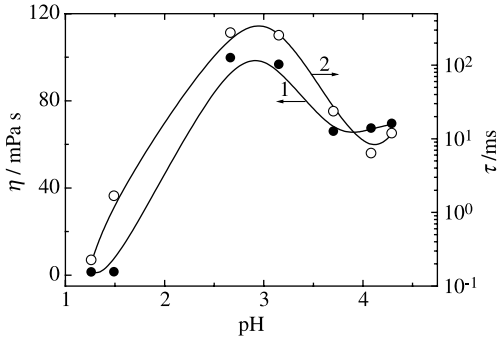

Fig. 9. Viscosity, η (curve 1) and DLS relaxation time, τ (curve 2), of the PS(20, 3k)–PVP(20, 23k) solution in aqueous HCl (copolymer concentration $c = 8.64$ g/l) prepared from the solution in 1,4-dioxane, as a function of pH. DLS was measured at scattering angle $\theta = 90°$.

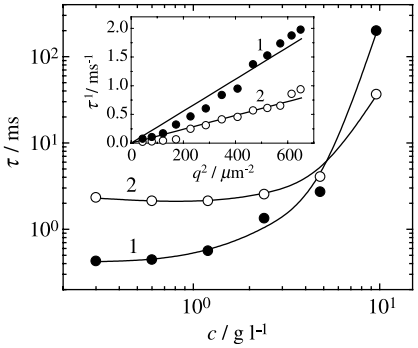

Fig. 10. Relaxation time, τ, evaluated from DLS (curve 1) and FCS (curve 2) measurement of PS(20,3k)–PVP(20,23k) solutions in 0.01 M HCl (prepared from the solution in 1,4-dioxane), as a function of copolymer concentration, c. DLS was measured at scattering angle $\theta = 90°$. Insert: Reciprocal DLS relaxation time, τ^{-1}, as a function of q^2, for two PS(20, 3k)–PVP(20, 23k) solutions in 0.01 M HCl. Copolymer concentrations were $c = 2.42$ g/l (curve 1) and $c = 4.83$ g/l (curve 2).

the observed behavior requires great care and caution. With respect to any premature conclusions, it is necessary to keep in mind that DLS intensities are the z-averages and overestimate the scattering from aggregates. Hence the presence of non-negligible fractions of freely moving single stars does not have to be detected in solutions containing bulky aggregates.

3.2. Fluorescence correlation spectroscopy and atomic force microscopy study

As mentioned above, static light scattering, SLS, yields the weight-average molar masses and z-average radii of gyration and the dynamic light scattering, DLS, measures the z-average based hydrodynamic radii. Both techniques are extremely sensitive to the presence of large and heavy particles in the solution (even to their traces). This sensitivity is generally an advantage for self-assembly studies, but in our case, when the studied system contains mostly unimers, it may obscure or disguise some important features of the behavior. It is why we applied two techniques which yield the number average data: (i) fluorescence correlation spectroscopy for measurement of M_n and the number-average based hydrodynamic radii, $(R_H^{-1})_n$ and (ii) atomic force microscopy for imaging micelles deposited on mica surface.

The number average molar masses, M_n, of unimer and multimolecular micelles were evaluated from the number of fluorescent particles in the irradiated volume, obtained from the FCS measurement with aqueous solutions of PS(20, 3k)–PVP(20, 23k) labeled with octadecylrhodamine B, as described in our earlier paper [25]. The number average based hydrodynamic radii, i.e. the values $(R_H^{-1})_n$, were obtained by fitting the autocorrelation curve of fluorescence fluctuations to a model curve assuming possible presence of two distinct fluorescence species (fluorescently labeled polymer and free probe) in the solution as described in

detail in our earlier study [25]. FCS data are summarized in Table 1. Even though the latter measurement is less precise than the former and may be influenced by a systematic calibration error (i.e. by changes in the irradiated volume with time) and by simplifications used in the derivation of the autocorrelation function, the trends in measured values are correct. The FCS results support the conclusion that aqueous solutions prepared from 1,4-dioxane–methanol (0–60 vol%) mixtures, contain mostly unimers.

Further, we measured the apparent diffusion time of strongly interacting unimer stars in aqueous solutions as a function of copolymer concentration. In Fig. 10, the results for the solution at pH 2 are compared with diffusion times obtained by DLS. Both curves show an increase in diffusion times with increasing concentration, but the increase is less pronounced for FCS data, which is reasonable because FCS measures the number-averages. Hence we believe that the difference is probably due to the polydispersity of temporary aggregates.

For the AFM studies, the polymer particles (i.e. stars, aggregates, their mixtures) were deposited from aqueous solutions on the fresh mica surface. Micelles or stars are pancake-deformed upon their deposition on the surface, but we found in our earlier studies that the size of deposited nanoparticles is proportional to that in the solution [25]. By scanning a sufficiently large area covered by micelles, the number average distribution of molar masses may be reasonably evaluated. Fig. 11(a) shows a top view of the PS(20, 3k)–PVP(20, 23k) stars deposited on the freshly peeled-off mica surface from an aqueous solution with pH 2. Narrow distributions of micellar radii, R, heights, z, and molar masses, M_i, based on the section analysis of several hundreds of deposited micelles (for details see [25]) are reproduced in Fig. 10(b)–(d), respectively. A small number-averaged radius of deposited nano-objects ($R_n = 22.4$ nm) compares well with the calculated radius of unimer stars, which is 19 nm for the given number averaged height, $z_n = 1.2$ nm. The difference between the observed and the calculated radii can be attributed to finite tip size effect. Hence we can conclude that AFM images mostly the unimer stars deposited on the surface from the solution with a negligible admixture of fairly small aggregates.

Table 1
Characteristics of PS(20, 3k)–PVP(20, 23k) micelles measured by FCS

ϕ_{MeOH}[a]	$M_w \times 10^{-6}$ (g/mol)[b]	R_H (nm)[c]
0.0	0.5	28
0.5	0.5	38
1.0	2.5	86

Measured in 0.1 M HCl solutions prepared from solutions in 1,4-dioxane, 1, 4-dioxane–methanol mixture and methanol.
[a] Volume fraction of methanol.
[b] Molar mass.
[c] Hydrodynamic radius.

3.3. Steady-state and time-resolved fluorometry study

In our previous paper [4], we studied micropolarity and microheterogeneity of various PS(n, L_1)–PVP(n, L_2) heteroarm star copolymer micelles using pyrene as a fluorescent probe. The first vibrational band (372 nm) in pyrene emission spectrum corresponds to a symmetry-forbidden transition and occurs only due to interactions with surrounding molecules, while the third vibrational band (383 nm) is not influenced by the microenvironment. Therefore, the ratio of intensities at 372 and 383 nm, I_1/I_3, is frequently used for monitoring the polarity of the microenvironment of the dispersed and solubilized pyrene [47,48].

Winnik et al. [49] reported that the I_1/I_3 values for pyrene solubilized either in pure PS or in PS–PVP films are almost the same (about 1.1), whereas that in PVP film is substantially higher, about 1.5. This observation indicates that pyrene is considerably more soluble in polystyrene than in polyvinylpyridine. This is in accordance with our measurements with PS(n, L_1)–PVP(n, L_2) micelles, where we found I_1/I_3 values about 1.1 which correspond rather to polystyrene than to PVP, despite the fact that about 40% of PVP monomeric units in micelles are not protonized and form relatively hydrophobic nanodomains.

In this study, we measured the I_1/I_3 values and time-resolved I_3 fluorescence decays for solutions of PS(20, 3k)–PVP(20, 23k) micelles transferred in 0.1 M HCl by dialysis. The I_1/I_3 ratio is almost the same both for unimers and for systems containing unimers and multimolecular micelles (Table 2). This observation is interesting because the studied copolymer cannot form multimolecular micelles with the fully segregated PS cores and PVP shells. However, the fluorescence measurements suggest that the PS domains in the core are large enough to solubilize pyrene and to screen it from interactions with PVP chains. Pyrene has very long fluorescence lifetime and is extremely sensitive to various dynamic quenching processes. We measured fluorescence decays from pyrene solubilized in some PS(20, 3k)–PVP(20, 23k) unimer and micellar systems. Fitting the decays to the double exponential model provides

Table 2
Characteristics of the fluorescence from pyrene solubilized in PS(20, 3k)–PVP(20, 23k) micelles

ϕ_{MeOH}[a]	I_1/I_3[b]	τ_1 (ns)[c]	τ_2 (ns)[c]	F_2[c]
0.0	1.11	341	70	0.094
0.5	1.11	344	57	0.089
1.0	1.12	355	70	0.062

Measured in 0.1 M HCl solutions prepared from solutions in 1,4-dioxane, 1, 4-dioxane–methanol mixture and methanol. Excitation at 336 nm, copolymer concentration 1.5 g/l, pyrene concentration 5 μM.
[a] Volume fraction of methanol in the starting solution.
[b] Ratio of fluorescence intensities at 372 and 383 nm (the first and the third vibration bands).
[c] Parameters of the double-exponential fit of the fluorescence decay at 383 nm; $I_F(t) \sim [(1-F_2)/\tau_1]\exp(-t/\tau_1) + [F_2/\tau_2]\exp(-t/\tau_2)$.

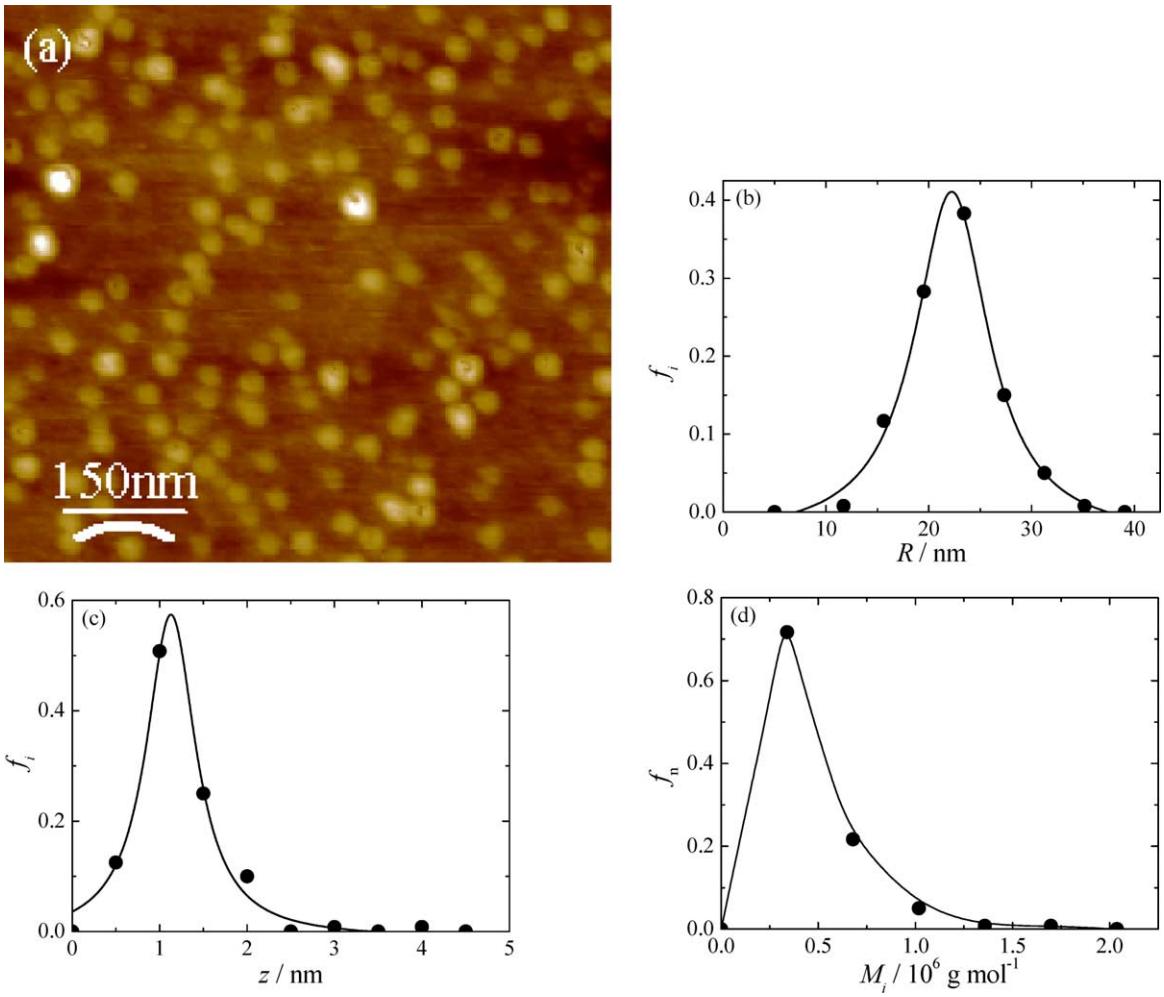

Fig. 11. (a) AFM scan (top view) of PS(20, 3k)–PVP(20, 23k) stars deposited on mica surface from an aqueous solution with pH 2 (prepared from the solution in 1,4-dioxane) and distribution functions of (b) radius, R, (c) height, z and (d) molar mass, M_i.

random distributions of residuals and χ^2 values less than 1.05. The fluorescence decay parameters are listed in Table 2. The fraction of quenched fluorescence, represented by the shorter decay component (65 ns on average) is approx. 6% in large multimolecular micelles prepared from methanol and approx. 9% in unimer stars. A stronger pyrene fluorescence quenching in unimers than that in multimolecular micelles supports the conclusion that the center of PS(20, 3k)–PVP(20, 23k) unimer star is less compact as compared with multimolecular micelles.

3.4. Comparison of the observed behavior with that of other charged star and micellar systems

As concerns the polyelectrolyte behavior, both 'hairy' PS–PVP heteroarms with partially protonized PVP arms and spherical PS–PMA micelles with partially dissociated PMA shell-forming blocks (that we studied recently [35]) behave as charged nanoparticles which strongly interact electrostatically over fairly long distances in low ionic strength solutions. In both systems, the initial slopes of q^2-dependences in the Zimm plots are negative and the viscosity of solutions at concentrations more than 5 g/l changes strongly and non-monotonously with ionic strength. However, we did observe non-negligible differences between PS–PMA and PS–PVP. Recently published measurements for PS–PMA micelles in salt free solutions showed a strong tendency to form a 'lattice-like' long-range structural arrangement, even in dilute solutions when individual micelles are separated by relatively large distances [35]. In this study, the SLS and DLS data suggest possible formation of clusters of PS–PVP heteroarm stars at high concentrations, but the tendency to create a 'lattice-like' arrangement of stars at medium concentrations was not detected.

The main difference is due to the fact that a non-negligible ionization of PS–PVP stars occurs at pH lower than 3, when the ionic strength and electrostatic screening plays quite important role. Further differences are due to different sizes, different ranges of number concentrations (for similar weight concentrations) and different effective charges of scattering particles. Both systems are weak

polyelectrolytes and the actual ionization depends on conditions, but small heteroarm stars bear lower effective charge and do not interact over long distances as strong as large and potentially more chargeable micelles. Both systems are kinetically frozen, but the cores of PS–PMA micelles, which are formed by high numbers of fairly long and flexible PS blocks, are really glassy and they are surrounded by dense shell of long PMA blocks. The PS chains in heteroarm stars are fairly short and stiff. We do not assume the formation of a glassy core because the relatively stiff short PS chains cannot adopt suitable conformations in small central region. AFM measurements show that stars deposited on mica from water are flat including the central core region. This may be explained by the experimentally proven fact that the glass transition temperature of thin films is lower than that of bulk polymers [50]. In our earlier studies, we observed the deformation of small PS cores of micelles formed by low number of copolymers with long soluble chains by AFM [51], but we found that the bulky cores of micelles with high association number did not almost deform [25]. Since the cores of unimolecular micelles are surrounded by relatively lose shells, some minor aggregation during dialysis or even in aqueous solutions, which would enable better packing of PS chains, cannot be precluded. A careful analysis of AFM scans reveals also that predominantly unimers with a low admixture of aggregates have been deposited on mica from aqueous solutions of heteroarms at all concentrations.

It is interesting to compare the observed behavior of charged heteroarm stars with that of other branched polyelectrolytes and with polyelectrolyte micelles. Behavior of branched polyelectrolytes has been less studied than that of linear ones, but still a number of experimental and theoretical papers have been published on that subject (e.g. Refs. [52–54]). Theoretical studies predict that the conformations of branched polyelectrolytes should be less sensitive to changes in ionic strength, however, the basic trends are similar to those of linear ones [52]. Experimental studies focus mainly on two topics: (i) sizes and the static structure of stars (or micelles) in the solution in a wide range of concentrations [53] and (ii) their rheological behavior [54]. As concerns the first group of studies, the authors usually report that the size of stars (or micellar shells) shrinks with the addition of low-molar-mass salt (in the range of moderate salt concentrations, i.e. in the osmotic brush-like region) and that the polyelectrolyte effects in salt-free solutions are strongly pronounced for stars with a low number of arms, because the density of the fixed charges (of ionized groups at the polymer chain) is low and counterions escape more easily in bulk solution. These findings are in agreement with our observations (made in this and in a number of our earlier studies) [4,19,35].

In this paper, we did not study the rheology of aqueous solutions in detail. Viscometric measurements were performed only as a secondary support of our conclusions, because the pronounced viscosity changes with HCl concentration were the most obvious indicator of the role of electrostatic forces. However, it is interesting to compare our data with the rheology study of branched charged system by Antonietti et al. [54], because DLS and FCS correlation times reflect the velocity of the motion of polymeric particles and report on their effective size and the friction of the medium, similarly as viscosity does. The authors performed a careful analysis of concentration dependence of the reduced viscosity, η_{red}, of branched charged polymer solutions and interpreted the changes by considering the influence of electrostatic interactions on the single particle dynamics and by assuming the cooperative effects. The single particle effect was treated in terms of the Barker and Henderson perturbation theory [55], yielding the electrostatic potential-dependent effective hydrodynamic radius and the interparticle coupling was accounted for by the formula derived by Hess and Klein [56]. The authors identified three concentration regions: (a) in the low concentration region, $c < c^{**}$, each particle feels the electrostatic interactions of other particles, but the interparticle coupling is weak. The reduced viscosity increases and reaches maximum at c^{**}. (b) In the intermediate concentration range, the interparticle coupling, expressed in terms of the Hess and Klein theory, dominates the behavior and the reduced viscosity (proportional to the third power of the effective hydrodynamic radius) decreases. The reduced viscosity η_{red} scales with polymer concentration c as $\eta_{red} \propto c^{-0.25}$. (c) At a certain concentration c^*, the hydrodynamic equivalent spheres of individual heteroarm stars start to overlap and the reduced viscosity steeply increases.

As already mentioned, DLS and FCS correlation times, τ, reflect the velocity of diffusion motion and in the first rough approximation, they are expected to decrease slightly in the intermediate 'Hess and Klein' concentration region (scaling exponent ca. 0.08). However, the comparison is not straightforward. While the reduced viscosity is a macroscopic property of the system, the correlation time (even though the experimental value is the ensemble average) is a microscopic characteristics and is weighted differently than the viscosity data. Furthermore, our system is formed by heteroarm starts with hydrophobic PS arms and despite the fact that the unimer star is a stable prevailing form, the analysis of experimental data indicates a low fraction of associates in aqueous systems. Fig. 10 shows that FCS correlation times, which are number averages (more appropriate for comparison with viscosity data than DLS), are almost constant at low concentrations and start to grow up close to c^*. From this point of view, our data basically agree with the already published data. It seems that DLS, which is very sensitive to aggregation, 'sees' the formation of traces of aggregates in this concentration region. As already mentioned, the difference between absolute values of both techniques is due, in a minor part, to changes in the irradiated volume with time and, in a major part, to a simplified form of the FCS autocorrelation function. Even

though we use an advanced model [32], it does not include all potential complicating factors, e.g. the fact that scattering is instantaneous, while emission is separated from absorption by a time-window of tens nanosecond, has not been taken into account in the derivation of the autocorrelation function.

Hence we may conclude that the behavior of the studied system in the concentration region where the q^2-dependences of SLS data in the Zimm plots give negative slopes is dominated by the cooperative electrostatic interplay, but both DLS and FCS correlation times reflect the motion of individual charged particles. At high concentrations close to c^*, large and loose fluctuating shell-interacting clusters (or more and less concentrated regions) probably form in low ionic strength solutions.

4. Conclusions

The self-assembly of a 'hairy' heteroarm star copolymer with short PS and long PVP arms was studied in 1,4-dioxane–methanol mixture and in acidic aqueous media. SLS and DLS measurements show that the sample forms multimolecular micelles with a low association number in 1, 4-dioxane–methanol solvents with more than 20 vol% of methanol. The performed experiments suggest that the micellization obeys the closed association mechanism, even though the molar mass distribution of associates seems to be broad (broad distribution of relaxation times measured by DLS). The experimental techniques that provide the number-average characteristics (FCS and AFM) show that the number fraction of unimer is fairly high in mixed solvents (except pure methanol).

The reversible unimer-micelle systems may be transferred in acidic aqueous media by stepwise dialysis. During dialysis, the micellization equilibrium freezes. The comparison of SLS data measured before and after dialysis shows that the original unimer-micelle distribution is basically preserved. We do not assume that this is a general pattern of the micellization behavior of heteroarm stars but it is a result of the particular 'hairy' star architecture. The 'hairy' heteroarm stars structure promotes the solubility in water, which is manifested, e.g. by the possibility to transfer unimer stars from 1,4-dioxane to acidic water without any aggregation and other possible changes.

The light scattering measurements on low-ionic-strength solutions of unimer stars reveal strong electrostatic interaction between unimers containing protonized (charged) PVP arms and formation of aggregates at higher concentrations. In the light of the present findings the formation of a physical stiff gel observed in similar 'hairy' PS(24, 1.7k)–PANa(24, 14k) heteroarm stars in aqueous solution of relative low concentration (7.7 g/l) [2] should now be attributed to the same electrostatic effect. This is another interesting specific feature of these copolymers showing that they could also be used as efficient thickeners in aqueous formulations.

Acknowledgements

Karel Procházka, Zdeněk Tuzar and Miroslav Štěpánek acknowledge the financial support of the Grant Agency of the Czech Republic (Grants No. 203/04/0490 and 203/02/D048, respectively), Pavel Matějíček, Jana Humpolíčková and Jitka Havránková the support of the Ministry of Education of the Czech Republic (FRVŠ 1894/2004, 1901/2004 and 1899/2004, respectively). The authors thank the Marie Curie Research and Training Network (Grant No. 505 027, POLYAMPHI) for the support.

References

[1] Tsitsilianis C, Voulgaris D. Macromol Chem Phys 1997;198:997.
[2] Voulgaris D, Tsitsilianis C. Macromol Chem Phys 2001;202:3284.
[3] Vlahos CH, Horta A, Freire JJ. Macromolecules 1992;25:5974.
[4] Tsitsilianis C, Voulgaris D, Štěpánek M, Podhájecká K, Procházka K, Tuzar Z, et al. Langmuir 2000;16:6868.
[5] Huang Y, Bu LW, Zhang DZ, Su CW, Xu ZD, Bu LJ, et al. Polym Bull 2000;44:301.
[6] Pispas S, Hadjichristidis N, Potemkin I, Khokhlov A. Macromolecules 2000;33:1741.
[7] Wang XS, Winnik MA, Manners I. Macromol Rapid Commun 2003; 24:403.
[8] Sotiriou K, Nannou A, Velis G, Pispas S. Macromolecules 2002;35: 4106.
[9] Cai YL, Burguiere C, Armes SP. Chem Commun 2004;7:802.
[10] Yamauchi K, Takahashi K, Hasegawa H, Iatrou H, Hadjichristidis N, Kaneko T, et al. Macromolecules 2003;36:6962.
[11] Guo YM, Pan CY. Polymer 2001;42:2863.
[12] Beyer FL, Gido SP, Uhrig D, Mays JW, Tan NB, Trevino SF. J Polym Sci, Polym Phys 1999;37:3392.
[13] Floudas G, Hadjichristidis N, Iatrou H, Pakula T, Fischer EW. Macromolecules 1994;27:7735.
[14] Werts MPL, Van der Vegte EW, Grayer V, Esselink E, Tsitsilianis C, Hadziioannou G. Adv Mater 1998;10(6):452.
[15] Kiriy A, Gorodyska A, Minko S, Stamm M, Tsitsilianis C. Macromolecules 2003;36:8704.
[16] Webber SE, Munk P, Tuzar Z, editors. Solvents and self-organization of polymers. NATO ASI series. Dordrecht: Kluwer Academic Publishers; 1996.
[17] Hamley IW. Physics of block copolymers. Oxford: Oxford University Press; 1998.
[18] Tuzar Z, Kratochvíl P. In: Matijevic E, editor. Surface and colloid science, vol. 15. New York: Plenum Press; 1993.
[19] Procházka K, Martin TJ, Munk P, Webber SE. Macromolecules 1996; 29:6518.
[20] Shen WH, Eisenberg A. Macromolecules 2000;33:2561.
[21] Butun V, Lowe AB, Billingham NC, Armes SP. J Am Chem Soc 1999;121:4288.
[22] Wooley KL. J Polym Sci, Polym Chem 2000;38:1397.
[23] Regenbrecht M, Akari S, Förster S, Mohwald H. J Phys Chem B 1999; 103:6669.
[24] Matějíček P, Uhlík F, Limpouchová Z, Procházka K, Tuzar Z, Webber SE. Macromolecules 2002;35:9487.
[25] Matějíček P, Humpolíčková J, Procházka K, Tuzar Z, Špírková M, Hof M, et al. J Phys Chem B 2003;107:8232.

[26] Jakeš J. Czech J Phys 1988;B38:1305.
[27] Papanastasiou GE, Ziogas II. J Chem Eng Data 1992;37:167.
[28] Kratochvíl P. In: Jennkins AD, editor. Classical light scattering from polymer solutions. Polymer science library, vol. 5. Amsterdam: Elsevier; 1987.
[29] Tuzar Z, Kratochvíl P. Collect Czech Chem Commun 1967;32:3358.
[30] Brandup J, Immergut EH, editors. Polymer handbook. 3rd ed. New York: Wiley Interscience; 1989.
[31] Webb WE. In: Riedler R, Elson ES, editors. Fluorescence correlation spectroscopy theory and applications. Berlin: Springer; 2001.
[32] Hink MA, van Hoek A, Visser AJWG. Langmuir 1999;15:992.
[33] Havránková J, Limpouchová Z, Procházka K. Macromol Theory Simul 2003;12:512.
[34] Elias H-G. In: Huglin NB, editor. Light scattering from polymer solutions. London: Academic Press; 1972.
[35] Matějíček P, Podhájecká K, Humpolíčková J, Uhlík F, Jelínek K, Limpouchová Z, et al. Macromolecules 2004;37:10141.
[36] Pincus P. Macromolecules 1991;24:2912.
[37] Israels R, Leermakers FAM, Fleer GJ, Zhulina EB. Macromolecules 1994;27:3249.
[38] Borisov OV, Zhulina EB, Birshtein TM. Macromolecules 1994;27:4795.
[39] Shusharina NP, Linse P, Khokhlov AR. Macromolecules 2000;33:3892.
[40] Misra S, Mattice WL, Napper DH. Macromolecules 1994;27:7090.
[41] Borisov OV, Zhulina EB. Macromolecules 2003;36:10029.
[42] Katchalski A. J Polym Sci 1951;7:393.
[43] Anufrieva EV, Birshtein TM, Nekrasova TN, Ptitsyn CB, Scheveleva TV. J Polym Sci C 1968;16:3519.
[44] Ghiggino KP, Tan KL. In: Phillips D, editor. Polymer photophysics. London: Chapman and Hall; 1985 [chapter 7].
[45] Wang YC, Morawetz H. Macromolecules 1986;19:1925.
[46] Schurtenberger P. In: Lindner P, Zemb T, editors. Neutrons, X-rays and light: scattering methods applied to soft condensed matter. Amsterdam: North-Holland; 2002 [chapter 11].
[47] Kalyanasundaram K, Thomas JK. J Am Chem Soc 1977;99:2039.
[48] Grohn F, Antonietti M. Macromolecules 2000;33:5938.
[49] Nakashima K, Winnik MA, Dai KH, Kramer EJ, Washiyama J. Macromolecules 1992;25:6866.
[50] Pham JQ, Green PF. Macromolecules 2003;36:1665.
[51] Štěpánek M, Humpolíčková J, Procházka K, Hof M, Tuzar Z, Špírková M, et al. Collect Czech Chem Commun 2003;68:2120.
[52] Wolterink JK, Leermakers FAM, Fleer GJ, Koopal LK, Zhulina EB, Borisov OV. Macromolecules 1999;32:2365.
[53] Moinard D, Taton D, Gnanou Y, Rochas C, Borsali R. Macromol Chem Phys 2003;204:89.
[54] Antonietti M, Briel A, Förster S. Macromolecules 1997;30:2700.
[55] Barker JA, Henderson D. Annu Rev Phys Chem 1972;23:439.
[56] Hess W, Klein R. Adv Phys 1983;32:173.